JBC RESEARCH ARTICLE

Disruption of the cholinergic anti-inflammatory response by R5-tropic HIV-1 protein gp120$_{JRFL}$

Received for publication, January 4, 2020, and in revised form, March 24, 2021 Published, Papers in Press, March 31, 2021,
https://doi.org/10.1016/j.jbc.2021.100618

Sonnieliz Cotto Ríos[1], José O. Colón Sáez[2], Orestes Quesada[3], Katherine Quiroz Figueroa[4], and José A. Lasalde Dominicci[1,4,5,6,*]

From the[1]Department of Chemistry, University of Puerto Rico, Río Piedras Campus, San Juan, Puerto Rico, USA; [2]Department of Pharmaceutical Sciences, University of Puerto Rico, Medical Sciences Campus, San Juan, Puerto Rico, USA; [3]Department of Physical Sciences and [4]Department of Biology, University of Puerto Rico, Río Piedras Campus, San Juan, Puerto Rico, USA; [5]Institute of Neurobiology, University of Puerto Rico Medical Science Campus, San Juan, Puerto Rico, USA; and [6]Molecular Sciences Research Center, University of Puerto Rico, San Juan, Puerto Rico, USA

Despite current pharmacological intervention strategies, patients with HIV still suffer from chronic inflammation. The nicotinic acetylcholine receptors (nAChRs) are widely distributed throughout the nervous and immune systems. In macrophages, activation of alpha7-nAChR (α7-nAChR) controls inflammatory processes through the cholinergic anti-inflammatory response (CAR). Given that this innate immune response controls inflammation and α7-nAChR plays a critical role in the regulation of systemic inflammation, we investigated the effects of an R5-tropic HIV soluble component, gp120$_{JRFL}$, on the CAR functioning. We previously demonstrated that X4-tropic HIV-1 gp120$_{IIIB}$ disrupts the CAR as well as inducing upregulation of the α7-nAChR *in vitro* in monocyte-derived macrophages (MDMs), which correlates with the upregulation observed in monocytes, T-lymphocytes, and MDMs recovered from HIV-infected people. We demonstrate here using imaging and molecular assays that the R5-tropic HIV-1 glycoprotein gp120$_{JRFL}$ upregulates the α7-nAChR in MDMs dependent on CD4 and/or CCR5 activation. This upregulation was also dependent on MEK1 since its inhibition attenuates the upregulation of α7-nAChR induced by gp120$_{JRFL}$ and was concomitant with an increase in basal calcium levels, which did not result in apoptosis. Moreover, the CAR was determined to be disrupted, since α7-nAChR activation in MDMs did not reduce the production of the proinflammatory cytokines IL-6, GRO-α, or I-309. Furthermore, a partial antagonist of α7-nAChR, bupropion, rescued IL-6 but not GRO-α or I-309 production. Together, these results demonstrate that gp120$_{JRFL}$ disrupts the CAR in MDMs. Other medications targeting the α7-nAChR need to be tested to reactivate the CAR to ameliorate inflammation in HIV-infected subjects.

Worldwide, approximately 36.7 million people are HIV-positive, with 1.8 million new cases reported and 1.0 million AIDS-related deaths in 2016 alone (http://www.unaids.org/en/topic/data). The human immune deficiency virus type 1 (HIV-1) accomplishes cell entry by direct interaction between the viral envelope glycoproteins gp120 and gp41 with the CD4 receptor present in the host's target cells. This interaction results in conformational changes on the gp120-CD4 receptor complex, enabling the virus to interact with either the CXCR4 coreceptor or CCR5 and culminating in the gp41-mediated fusion between the viral envelope to finally infect the target cell (1).

Macrophages are one of the key HIV-1-targeted cells that can be infected by M-tropic strains through the CCR5 (R5-tropic strain) coreceptor or by dual-tropic (X4/R5) strains that use both coreceptors for cell infection (2, 3). Importantly, because HIV-1 M-tropic strains (R5 strains) appear to play an essential role in HIV spread (4), it is crucial to understand how signaling triggered by soluble viral constituents (*e.g.*, gp120), acting through the CCR5 receptor, affects the inflammatory phenotype of macrophages, and how these cells could be targeted pharmacologically to activate an innate anti-inflammatory mechanism, called the cholinergic anti-inflammatory response (CAR), to treat the chronic inflammation suffered by HIV-infected subjects.

Since 2000, special attention has been paid to the CAR as an innate neuroimmune mechanism that regulates and controls excessive inflammation. This is a prototypical neural circuit activated peripherally by cytokines and inflammatory products (5, 6). This anti-inflammatory mechanism is dependent on the signal transduction *via* macrophages alpha7 nicotinic acetylcholine receptor (α7-nAChR), which binds acetylcholine (ACh) to inhibit the production of inflammatory cytokines without altering IL-10 levels (7). Although there is robust evidence on the benefits of activating this anti-inflammatory mechanism to counteract inflammation, in the field of HIV there are practically no studies focused on this topic except for evidence recently reported by our group (8).

Indeed, studies performed in our laboratory using the X4-derived viral envelope gp120$_{IIIB}$ show that activation of the CXCR4 by this viral glycoprotein increases the expression of α7-nAChR in human monocyte-derived macrophages (MDMs) (8, 9). Interestingly, this upregulation was also observed in T-lymphocytes, monocytes, and macrophages from HIV-infected patients (8). However, in this upregulated setting, α7-nAChR activation failed to inhibit the production

* For correspondence: José A. Lasalde Dominicci, jose.lasalde@upr.edu.
Present address for Katherine Quiroz Figueroa: Department of Microbiology, Perelman School of Medicine at the University of Pennsylvania, Philadelphia, PA.

of the majority of proinflammatory cytokines in MDMs deliberately pre-exposed to gp120$_{IIIB}$ followed by lipopolysaccharide (LPS) challenges. These results suggest that gp120$_{IIIB}$ disrupts an innate immune response mechanism that controls inflammation in HIV-infected subjects, the CAR. Moreover, these results underscore the importance of better understanding the mechanism behind the gp120-induced α7-nAChR upregulation, which may be associated with an unresolved problem in the HIV field: chronic inflammation. Although important advances have been made concerning the consequences of the X4-tropic gp120$_{IIIB}$ on macrophage's α7-nAChR expression and the CAR (8), the repercussions of the R5-tropic gp120$_{JRFL}$ on the α7-nAChR expression and the CAR operation in MDMs are still unknown.

In the current work, we found that gp120$_{JRFL}$ induced the upregulation of α7-nAChR in MDMs results that are consistent with those reported previously using gp120$_{IIIB}$ (8). Also, α7-nAChR's baseline levels correlated with the magnitude of the observed upregulation. Moreover, the α7-nAChR upregulation was significantly reduced after blocking CCR5 and CD4 receptors, suggesting that stimulation of these receptors could lead to α7-nAChR upregulation in these cells. Furthermore, CCR5 endogenous agonists RANTES and MIP-1β also abrogated gp120$_{JRFL}$-induced upregulation of α7-nAChR, suggesting that activation of CCR5 or CD4 could trigger α7-nAChR upregulation in human macrophages. Also, α7-nAChR upregulation was attenuated by a MEK1 inhibitor and did not depend on *de novo* protein synthesis. Moreover, we found that the addition of gp120$_{JRFL}$ to MDMs promoted higher basal calcium levels, but not apoptosis. These cellular and molecular results underscore the molecular complexity behind the gp120-induced α7-nAChR upregulation in MDMs. Of note, from the inflammation standpoint, we found a CAR disruption for cytokines IL-6, GRO-α, and I-309, but not for TNF-α. Additionally, treatment with bupropion, a partial antagonist of α7-nAChR, reestablished the CAR for only IL-6, not the other cytokines.

Results

R5-tropic HIV-1 gp120$_{JRFL}$ upregulates the α7-nAChR in MDMs

To study the effects of the R5-tropic gp120$_{JRFL}$ on α7-nAChR's expression, MDMs were treated with different concentrations of gp120$_{JRFL}$ including those within the pathophysiological range (0.002–2.5 nM) found in HIV-infected patients (10–13). Binding assays were performed using Alexa-488-α-bungarotoxin (α-BuTX) to detect surface expression of α7-nAChR in MDMs upon gp120$_{JRFL}$ exposure (Fig. S1*A*). As shown in Figure 1*A*, gp120$_{JRFL}$ at different concentrations (0.15 and 150 nM) significantly increased binding of α-BuTX in MDMs, suggesting higher levels of α7-nAChR. Moreover, Figure 1*B* shows that following exposure to a pathophysiological concentration (0.15 nM) of gp120$_{JRFL}$, there was a significant increase in α-BuTX binding in nine of the total 14 donors (p = 0.0134, 64%). Not all donors exhibited elevated levels of α7-nAChR, possibly owing to genetic variations (14–16) between individuals, which are common in macrophages (8). Also, the upregulation detected for α7-nAChR in MDMs was directly proportional to the baseline levels that each donor had (Fig. S2), similar to what has been previously reported for g120$_{IIIB}$ (8). Upregulation results were confirmed by immunoblot assays that also showed increased levels of α7-nAChR in gp120$_{JRFL}$-treated MDMs (Fig. 1*F*). Since this study focused on the mechanism and effects of gp120$_{JRFL}$-induced α7-nAChR upregulation in the inflammatory response of MDMs, from this point forward (Fig. 1) all analyses were done using donors who demonstrated α7-nAChR upregulation in their respective MDMs upon gp120$_{JRFL}$ exposure. Consistent with previous studies we found that, as shown in Figure 1*C*, treatment with X4-tropic gp120$_{IIIB}$ increased the levels of α-BuTX binding in MDMs (8). Notably, similar results were observed after treatment with a different R5-tropic glycoprotein, gp120$_{JRFL}$ (Fig. 1*C*) and gp120$_{ADA}$ (Fig. 1*D*). Furthermore, to demonstrate the selective binding of α-BuTX to the α7-nAChR, nicotine competitive assays were performed in upregulated MDMs. As expected, results showed that nicotine pretreatment significantly reduced α-BuTX binding (Fig. 1*E*). Lastly, the increase in α7-nAChR levels occurred preceded by a nonsignificant increase in *Egr1* after 6 h of incubation with gp120$_{JRFL}$ (Fig. S3).

CCR5 mediates gp120$_{JRFL}$-induced upregulation of α7-nAChR in MDMs

Chemokine coreceptors, CXCR4 and CCR5, expressed on immune cells are important for HIV-1 virus entry into CD4 expressing cells. CCR5 is the principal coreceptor used by M-tropic strains (*e.g.*, gp120$_{JRFL}$) to infect macrophages while CXCR4 (*e.g.*, gp120$_{IIIB}$) is used by T-tropic virus strains to infect and replicate activated CD4$^+$ T-lymphocytes and macrophages (17, 18). Also, as mentioned, it has been shown that gp120$_{IIIB}$, through CXCR4, induces α7-nAChR upregulation in MDMs while HIV-infected individuals exhibit elevated levels of α7-nAChR in their monocytes, T-lymphocytes, and MDMs (8). Given these findings, we hypothesized that the CCR5 coreceptor could also be involved in the mechanism of gp120$_{JRFL}$-mediated upregulation of α7-nAChR in MDMs. Details of the treatments are presented in Figure S1*B*. As shown in Figure 2, *A* and *B*, the therapeutic CCR5 antagonist maraviroc prevented the increase of α-BuTX binding induced by gp120$_{JRFL}$. Similar results were obtained in MDMs pretreated with the CD4 receptor antagonist, 4,4′-diisothiocyanatostilbene-2,2′-disulfonic acid (DIDS) (Fig. 2, *A* and *B*). Interestingly, the CCR5 natural agonists MIP-1β and RANTES also prevented the increase in α-BuTX binding (Fig. 2, *A* and *B*), suggesting a reduction in the expression of surface α7-nAChR in MDMs. These suggest that gp120$_{JRFL}$ could potentially activate other mechanisms that also result in α7-nAChR upregulation. Together, these results highlight the importance of CD4 and CCR5 stimulation for the upregulation of α7-nAChR in MDMs.

gp120$_{JRFL}$-CCR5 interaction involves MAPK signaling in MDMs

Based on these findings, we next sought to investigate whether the signaling cascades resulting from gp120$_{JRFL}$ addition, shown to be dependent on activation of CD4 and

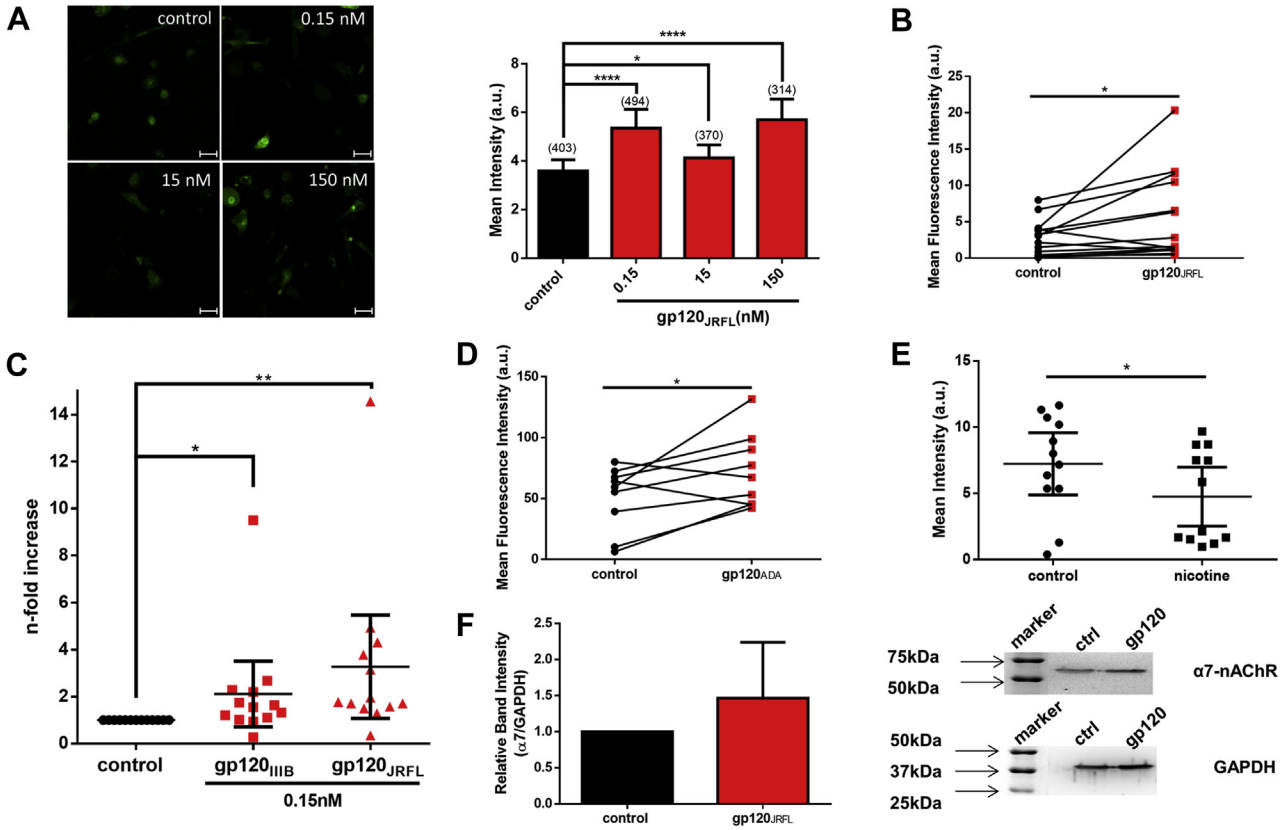

Figure 1. HIV-1 R5 gp120$_{JRFL}$ upregulates the α7-nAChR in MDMs. MDMs from uninfected subjects were used to evaluate α7-nAChR's expression. *A*, MDMs were treated with 0.15, 15, and 150 nM of gp120$_{JRFL}$ followed by α-BuTX addition. Scale bar: 20 μm. The total number of MDMs analyzed is in parenthesis at the top of each column. ****$p \leq 0.0001$, ***$p = 0.0002$ ($n = 5$ subjects). *B*, fourteen donors were evaluated for α7-nAChR levels after gp120$_{JRFL}$ (0.15 nM) exposure. Measurements were performed for each donor before and after gp120$_{JRFL}$ treatment. Mean fluorescence intensity measurements show a significant increase in α7-nAChR expression (*p= 0.0134). *C*, comparison of gp120$_{IIIB}$ (*$p = 0.0210$) and gp120$_{JRFL}$ (**$p = 0.0034$) effects on MDMs showed that α7-nAChR levels are higher in those incubated with gp120$_{JRFL}$ (0.15 nM). Untreated counterparts were normalized to 1, ($n = 13$ subjects). *D*, nine donors were evaluated for α7-nAChR levels after gp120$_{ADA}$ (0.15 nM) addition. Confocal imaging showed a significant increase in α7-nAChR levels expression (*p = 0.0273). *E*, nicotine outcompetes α-BuTX binding in MDMs demonstrating α-BuTX selectivity for α7-nAChRs, dots in graph represent snapshots, ($n = 4$ subjects, control $n = 132$ and nicotine-treated = 134 cells, *$p = 0.0274$). Each subject was identified using distinctive dots. *F*, immunoblot assays revealed that MDMs exposed to a pathophysiological concentration of gp120 (0.15 nM) exhibit higher α7-nAChR protein levels relative to their untreated counterparts normalized to 1 ($n = 3$ subjects). Incubation time for gp120$_{JRFL}$ was 72 h. Total protein amount was normalized to GAPDH signal. Lane 1: molecular weight markers, lane 2: untreated (ctrl) sample, and lane 3: gp120$_{JRFL}$-treated samples. Statistical analysis for *panel A* consists of a one-way ANOVA, *panel E* consists of a paired Student's *t*-test, and for *panels B*, *C*, and *D* analysis consists of a Wilcoxon's signed-rank test. Error bars represent mean with 95% CI for *panels A*, *C*, *F*, and *E*. Raw values were employed for *panels A*, *B*, *D*, and *E* while normalized values were used in *panels C* and *F*.

CCR5, activate MAPK signaling in MDMs. Previous findings have shown that the CXCR4 receptor agonist SDF-1α and gp120$_{IIIB}$ upregulate the *Egr1* gene, a transcription factor of α7-nAChR (18–20). To investigate further, we pretreated MDMs with PD98059, a highly selective inhibitor of MEK1, to prevent its activation (21). Details of the treatments are presented in Figure S1*C*. Our results show that α7-nAChR upregulation was attenuated by PD98059 pretreatment (Fig. 3, *A* and *B*), suggesting that gp120$_{JRFL}$ requires MAPK activation to upregulate α7-nAChR in MDMs. Unexpectedly, the addition of PD98059 alone did not reduce α7-nAChR to control levels. Taken together, these results suggest that gp120$_{JRFL}$ interaction with the CCR5 receptor activates MAPK signaling, which may promote the transcription of α7-nAChRs. However, protein synthesis inhibition results showed that the increase in α7-nAChR surface expression did not depend on *de novo* protein synthesis, suggesting that gp120$_{JRFL}$ could be affecting the trafficking of previously synthetized α7-nAChRs pool to the plasma membrane.

The CCR5 antagonist maraviroc did not rescue the CAR

Based on our findings, it seems that gp120$_{JRFL}$ activates a signaling cascade that depends on both CD4 and CCR5 stimulation, which is critical for gp120$_{JRFL}$-mediated upregulation of α7-nAChRs. Consequently, to evaluate the significance of CCR5 blockade in the CAR functioning, we used the therapeutic drug maraviroc. As mentioned, maraviroc prevented the α7-nAChR upregulation (Fig. 2*B*). Here, we tested whether blockade of CCR5 with maraviroc would help restore the CAR measuring cytokines produced by MDMs. Results showed that maraviroc did not reduce any of the cytokines measured (Fig. S4).

gp120$_{JRFL}$-mediated upregulation of α7-nAChR does not trigger apoptosis in MDMs

Several studies have proved that calcium overload through α7-nAChR (19, 22) and its uncontrolled influx induced by HIV-1 soluble proteins (23) can promote apoptosis in neurons (19, 22, 23). Considering that gp120$_{JRFL}$ can trigger

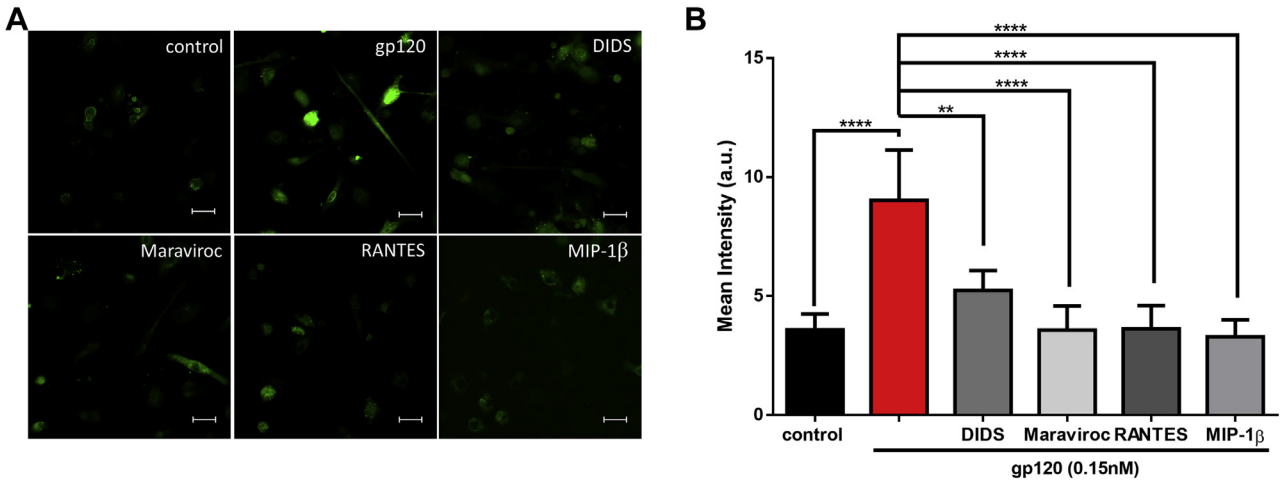

Figure 2. α7-nAChR upregulation by gp120$_{JRFL}$ is reduced after using selective CD4 receptor and CCR5 coreceptor antagonists. *A*, MDMs were first treated with DIDS (100 nM, CD4 antagonist) or maraviroc (100 nM, CCR5 antagonist) and RANTES (100 nM) or MIP-1β (100 nM) followed by exposure to gp120$_{JRFL}$ (0.15 nM). α7-nAChR expression levels were assessed using fluorescent α-BuTX. Confocal imaging studies and revealed that DIDS and maraviroc reduce α-BuTX binding to MDMs. Scale bar: 25 μm. *B*, α7-nAChR reduction was observed upon antagonist (DIDS and maraviroc) application. Also, addition of CCR5 agonists (RANTES and MIP-1β) reduces α7-nAChR expression. Incubation time for gp120$_{JRFL}$ was 72 h. Raw values were employed for *panel B*. Eight random snapshots were analyzed for each experimental condition/donor. The number of cells analyzed for each experimental condition were: control = 789, gp120 = 902, gp120 + DIDS = 482, gp120 + Maraviroc = 597, gp120 + RANTES = 786 and, gp120 + MIP-1β = 708. Scale bar: 20 μm. Error bars represent mean with 95% CI. *p = 0.0105, ****$p \leq 0.0001$. Wilcoxon matched-pairs signed-rank test, n = 7 subjects.

intracellular calcium signaling in macrophages through CCR5 stimulation and that α7-nAChRs are highly permeable to calcium, we studied possible changes in calcium after gp120$_{JRFL}$ exposure (24, 25) (Fig. S1*D*). As shown in Figure 4, *A* and *B*, gp120$_{JRFL}$ induced a significant increase in calcium basal levels in MDMs; however, the addition of the chelating agent, EGTA, or adding α-BuTX (an α7-nAChR blocker) did not result in a significant difference compared with responses to gp120$_{JRFL}$ alone (Fig. 4*B*). Furthermore, acetylcholine (ACh)-induced calcium mobilization after gp120$_{JRFL}$ addition, in MDMs upregulated for α7-nAChR, was not observed (data not shown). These findings suggest that α7-nAChR upregulation did not trigger apoptosis of macrophages, which is consistent with the antiapoptotic signature observed in HIV-infected monocytes (26, 27) and macrophages (28). Therefore, MDMs upregulated for the α7-nAChR did not undergo apoptosis upon ACh stimulation.

gp120$_{JRFL}$ disrupts the cholinergic anti-inflammatory response (CAR) in MDMs

Acute HIV-1 infection is associated with the induction of cytokine cascades, including interferon-α (IFN-α), interferon-γ (IFN-γ), inducible protein 10 (IP-10), TNF-α, IL-6, IL-10, and IL-15 (29). As a consequence, HIV-infected patients experience sustained and chronic inflammation that affects their immune status (30). Given the vital role of α7-nAChR in regulating innate immune responses through the CAR activation (31), we evaluated the cytokine profile of MDMs upregulated for α7-nAChR. Secretion of cytokines (interleukins and chemokines) was measured in MDMs challenged with LPS and exposed to gp120$_{JRFL}$ (Fig. S1*E*). As expected, ACh reduced the release of proinflammatory cytokines in LPS-treated MDMs (Fig. 5, *A* and *B*; green bars) not exposed to gp120$_{JRFL}$, indicating that the CAR is functional. Of

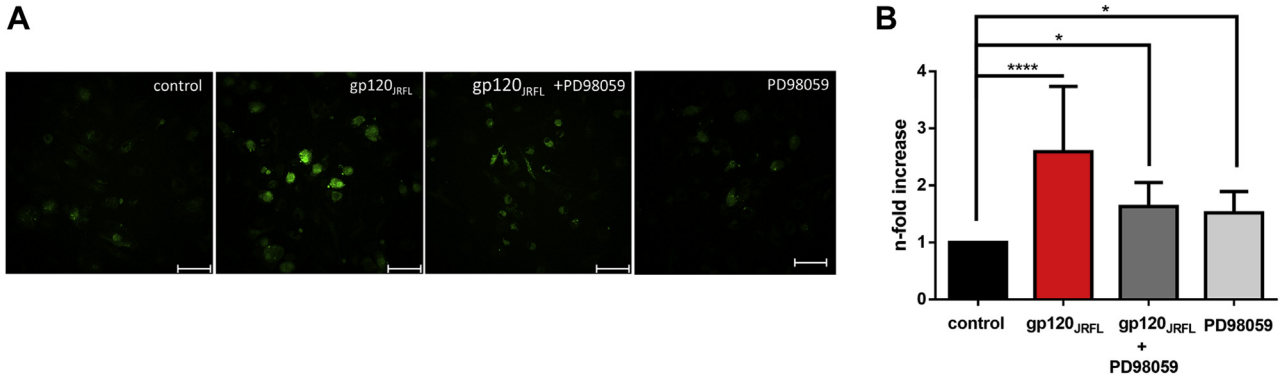

Figure 3. Upregulation of α7-nAChR involves MAPK signaling. *A*, MDMs were pretreated with the MEK1 inhibitor (PD98059, 10 μM) followed by gp120$_{JRFL}$ (0.15 nM) exposure. Then, α-BuTX binding assays were performed to measure α7-nAChR levels. Scale bar: 50 μm. *B*, PD98059 attenuates α-BuTX binding in MDMs exposed to gp120$_{JRFL}$. ***$p \leq 0.001$ and *p = 0.0367 (n = 6 subjects, the total number of cells analyzed for each experimental condition was: control = 1098, gp120$_{JRFL}$ = 1087, and gp120$_{JRFL}$ + PD98059 = 1177, PD98059 =1138). Cells from eight random snapshots were obtained for each experimental condition per subject. Controls were normalized to 1. Error bars represent mean with 95% CI. Statistical analysis employed for panel B. Incubation time for gp120$_{JRFL}$ was 7 2 h.

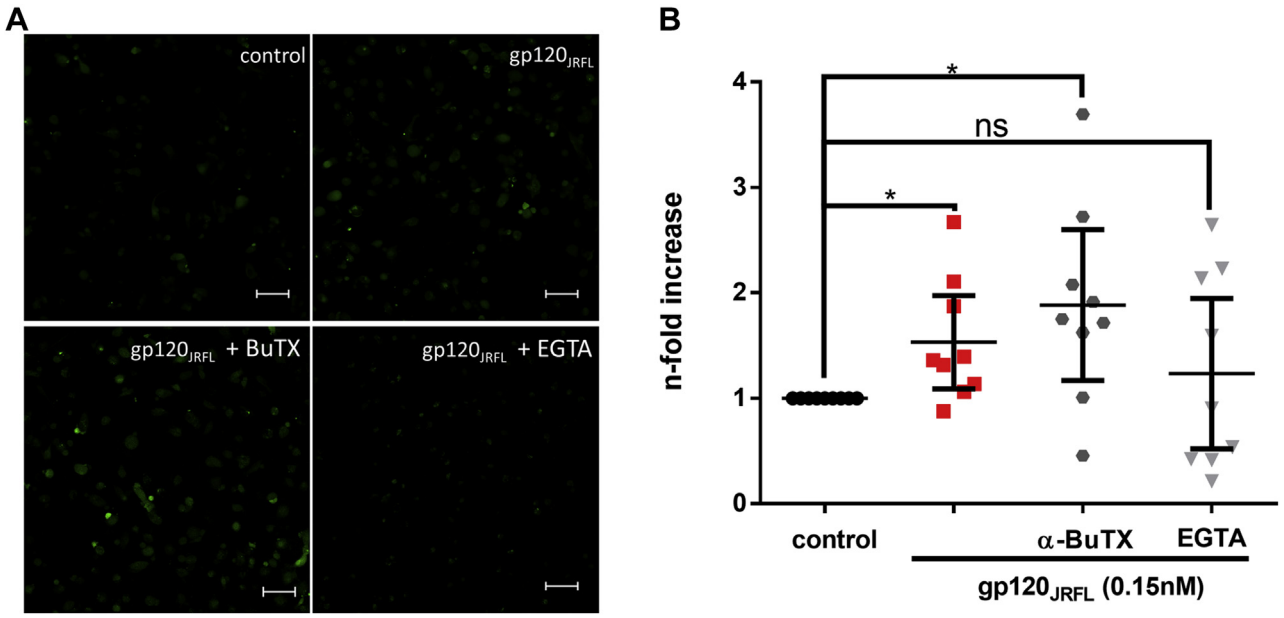

Figure 4. gp120$_{JRFL}$ increases basal calcium levels in MDMs upregulated for α7-nAChR. *A*, confocal imaging data suggest that gp120$_{JRFL}$ increased basal calcium levels. This increase was not prevented by extracellular calcium chelation using EGTA (10 nM) and α-BuTX (100 nM). Scale bar: 50 μm. *B*, calcium levels increased 1.5-fold after gp120$_{JRFL}$ exposure (α7-nAChR upregulation). Control (untreated) counterparts were normalized to 1. Error bars represent mean with 95% CI, *p = 0.0117. The total number of cells analyzed for each experimental condition was: control = 390, gp120$_{JRFL}$ = 364, gp120$_{JRFL}$ + α-BuTX = 316, and gp120$_{JRFL}$ + EGTA = 309. Incubation time for gp120$_{JRFL}$ was 72 h. A Wilcoxon matched-pairs signed-rank test (n = 3 subjects) was employed and its values were normalized.

note, ACh was able to reduce TNF-α production in LPS-treated MDMs upregulated for α7-nAChR (Fig. 5*A*) but not for IL-6. Also, as expected, CAR activation did not alter IL-10 levels (7). In terms of chemokines, ACh did not reduce the production of either GRO-α or I-309 in LPS-treated MDMs exposed to gp120$_{JRFL}$ (Fig. 2*B*). Therefore, in the presence of gp120$_{JRFL}$ (α7-nAChR upregulation), a CAR disruption was observed for the majority of cytokines tested. Overall, these results suggest that gp120$_{JRFL}$ negatively affected the CAR functioning in MDMs, thereby contributing to the inflammatory state present in HIV-infected subjects.

The α7-nAChR partial antagonist, bupropion limitedly restores the CAR

Considering that the α7-nAChR function is critical for proper CAR functioning (5), we next sought to determine whether it is possible to rescue the disrupted CAR pharmacologically. To this end, we pretreated MDMs with the α7-nAChR partial antagonist bupropion (32, 33), (Fig. S1*F*). We have previously shown that bupropion attenuates the production of some chemokines (MCP-1, RANTES, and GRO-α) in MDMs upregulated for α7-nAChR upon gp120$_{IIIB}$ addition followed by LPS challenging (8). As shown in Figure 6, bupropion significantly attenuated IL-6 levels while no reduction was observed in the other cytokines.

gp120$_{JRFL}$-induced α7-nAChR upregulation does not involve cross talk between the CCR5/CXCR4 coreceptors signaling

Macrophages can be infected by M-tropic strains that use only the CCR5 receptor or by dual-tropic (X4/R5) strains that use both receptors. Even though analysis of newly infected individuals has shown that HIV-1 R5 virus strains are predominant at the early stages of infection in 80% of patients, X4 strains appear later during the development of the disease in 40–50% of patients (34, 35). Studies conducted in CD4/CXCR4-expressing cells transfected with CCR5 have demonstrated that both receptors heterodimerize and associate with CD4, suggesting that this interaction may modulate HIV-1 coreceptor function. To evaluate possible signaling cross talk between both coreceptors, MDMs were exposed to gp120$_{IIIB}$ and gp120$_{JRFL}$ in the presence of their correspondent antagonists AMD3100 (CXCR4) and maraviroc (CCR5). MDMs treated with both gp120s showed an increase in α7-nAChR's expression similar to the upregulation induced by gp120$_{IIIB}$ or gp120$_{JRFL}$ alone (Fig. S4, *A* and *B*). However, antagonizing the CCR5 with AMD3100 or the CXCR4 receptor with maraviroc did not result in a reduction of α7-nAChR upregulation (Fig. S4*B*). These results suggest that gp120's effects on MDMs were not mediated *via* cross talk between CCR5 and CXCR4 coreceptors. However, we cannot rule out the possibility that there might some kind of cross talk *via* their respective signaling cascades.

Discussion

The most successful available pharmacological strategy to fight HIV infection is antiretroviral therapy (ART). Although ART has been beneficial in reducing the risk of developing AIDS, it is not effective at reducing the continuous inflammatory immune response mounted against soluble viral proteins (*e.g.*, gp120) and other HIV constituents. Moreover, even though certain combinations of ART have shown certain effectiveness in reducing inflammation, it is not sufficient to reinstate basal levels to those displayed by HIV-uninfected people (36) or to eradicate residual inflammation in this

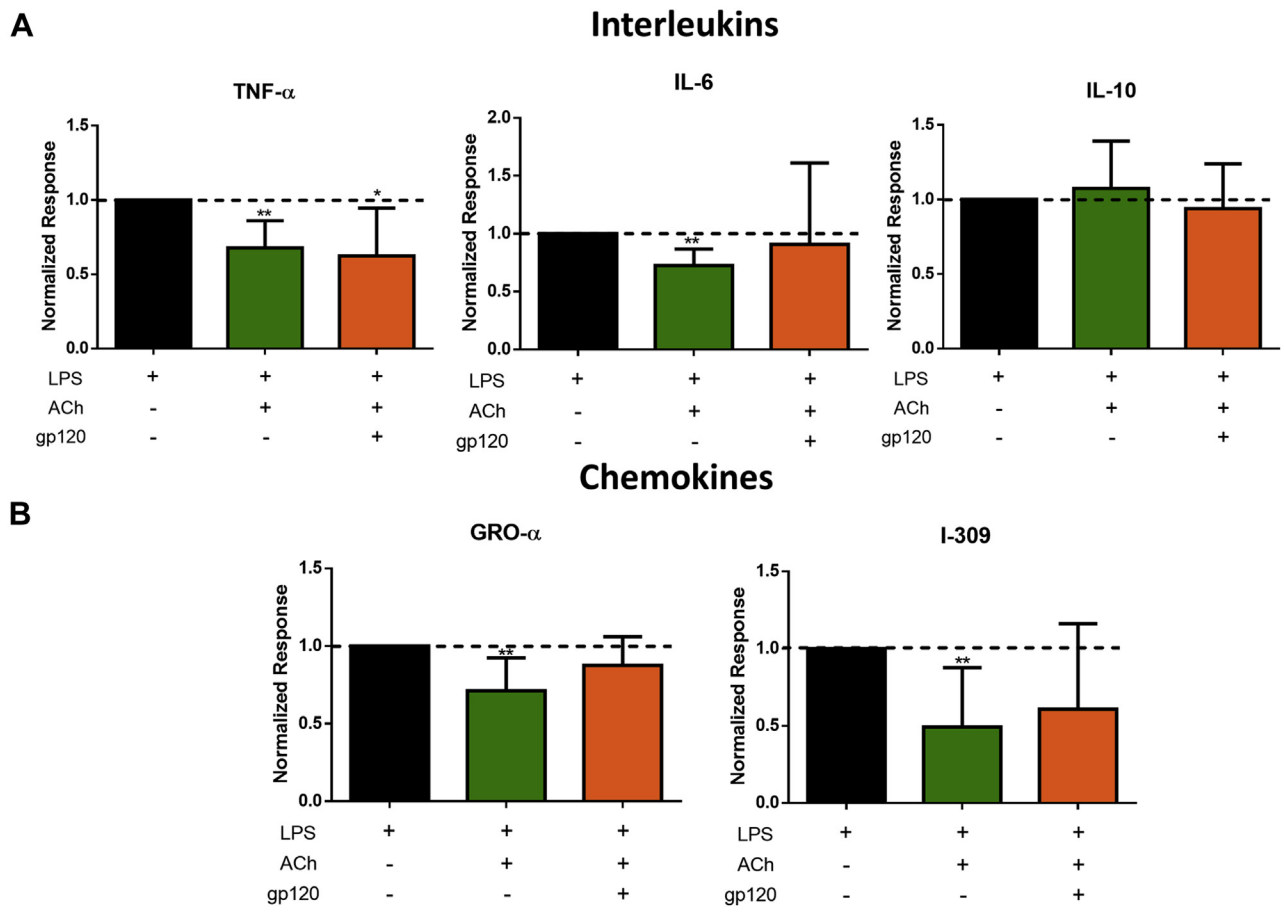

Figure 5. Effects of gp120$_{JRFL}$-induced upregulation of α7-nAChRs in MDM's CAR operation. *A*, interleukins quantification from MDMs showed that CAR activation upon addition of ACh significantly reduced proinflammatory cytokines release (*green bar*) without affecting IL-10 levels. However, IL-6 levels were not attenuated upon CAR activation in α7-nAChR upregulated MDMs. Also, pre-exposing MDMs to gp120$_{JRFL}$ (α7-nAChR upregulation) showed that TNF-α can be reduced upon CAR activation. *B*, chemokines quantification revealed CAR disruption for GRO-α and I-309. Results were normalized to LPS-induced cytokine release. Incubation time for gp120$_{JRFL}$ was 72 h. Normalized response equaled the cytokine concentration in the presence of LPS plus ACh divided by the concentration reached with LPS alone (LPS+ACh/LPS; *green bar*), and the cytokine concentration of MDMs upregulated for α7-nAChR in the presence of LPS plus ACh divided by the concentration reached by LPS alone ((LPS+ACh/LPS); *orange bar*). Statistical analysis used for both panels: One-sample *t*-test; n = 3–9 subjects. *$p \leq 0.05$; **$p \leq 0.01$, all values employed were normalized.

population (37). Recent results have shown that soluble gp120$_{IIIB}$ from an X4-tropic HIV-1 could disrupt an innate immune response (8, 9) tailored to decrease inflammation, the CAR, which operates through the α7-nAChR expressed by macrophages (5).

HIV soluble viral proteins such as gp120 circulate in the body of infected people and influence its physiology by interacting with receptors of immune cells, ultimately supporting and increasing the inflammatory process. In this study, the addition of gp120$_{JRFL}$ in concentrations similar to those present in HIV-infected patients (0.002–2.5 nM) (10–13) caused the upregulation of α7-nAChR in uninfected MDMs that depends on cells' basal expression levels. This upregulation was observed using pathophysiological (0.15 nM) and supraphysiological (15 and 150 nM) concentrations of gp120$_{JRFL}$ (Fig. 1*A*). Nevertheless, the extent of the α7-nAChR upregulation for the three concentrations tested proved to be similar among them (Fig. 1*A*), suggesting that upregulation reached a plateau. Interestingly, we did not observe statistically significant differences on α7-nAChR after applying an intermediate concentration (15 nM) of gp120$_{JRFL}$. This type of response is very similar to that observed before for gp120$_{IIIB}$ (8); however, this result does not influence the interpretation since both 15 and 150 nM are supraphysiological concentrations. On the other hand, the upregulation of α7-nAChR in MDMs using gp120s with different tropisms (X4: gp120$_{IIIB}$ and R5: gp120$_{JRFL}$ and gp120$_{ADA}$) was similar among them (Fig. 1, *C* and *D*). Interestingly, our Z-stack imaging studies and nicotine competitive binding assays confirm an observation previously made by other groups. We observed that the application of nicotine did not eliminate the fluorescent α-BuTX signal completely. This has been observed previously as α7-nAChR tends to accumulate intracellularly close to the perinuclear area in macrophages (5) and other cells expressing α7-nAChR (38–40). Overexpression of this high-calcium-permeable channel produced an increase in intracellular calcium levels but did not cause apoptosis, a finding similar to what has been observed for gp120$_{IIIB}$ (8) but opposite to what has been shown in neuronal cells (22). Thus, this may imply that neuronal cells are more susceptible to changes in calcium levels, suggesting

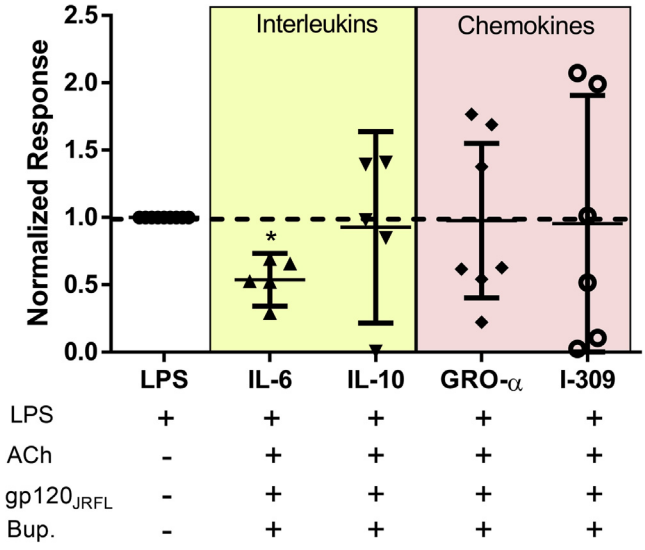

Figure 6. Bupropion limitedly restores the CAR in MDMs. α7-nAChR partial antagonist bupropion significantly decreased the levels of IL-6 but not the remaining cytokines in α7-nAChR upregulated MDMs. IL-10 levels remained unaltered. Results were normalized to LPS-induced cytokine release. Incubation time for gp120$_{JRFL}$ was 72 h. Normalized response equals the cytokine concentration in α7-nAChR upregulated MDMs in the presence of bupropion, LPS plus ACh, and divided by the concentration reached with LPS alone (Bup.+LPS+ACh/LPS). Statistical analysis was carried out using One-sample *t*-test; $n = 5$ to 7 subjects; $^*p \leq 0.05$, all values were normalized.

that the upregulation of α7-nAChR in the central nervous system has more serious consequences than it does in blood-derived macrophages. Our results suggest that the upregulation of α7-nAChR coincides with a greater calcium accumulation that does not come from extracellular sources, since chelation with EGTA did not decrease calcium entry. Similarly, the observed increase of MDM's intracellular calcium does not occur through α7-nAChR because blocking with α-BuTX did not prevent it.

Because extracellular calcium entry into MDMs does not occur *via* α7-nAChR, it is possible to occur through other mechanisms. Along these lines, recent studies demonstrated that α7-nAChR could interact with G-protein-coupled receptors once stimulated with acetylcholine (41–43). For instance, in T cells, mobilization of calcium through the α7-nAChR is not necessarily required for the nicotine-induced release of calcium from the internal stores (44). Moreover, channel-independent signal transduction has been related to the role of α7-nAChR in inflammation (45, 46). Another possibility is that the activation of CCR5 by gp120$_{JRFL}$ also allows calcium to accumulate in MDMs from intracellular stores, the latter has been demonstrated previously (25, 46). The fact that this increase in calcium was observed after adding gp120$_{JRFL}$ suggests that this glycoprotein may be activating CCR5, which is known to increase intracellular calcium levels (24). Nevertheless, this resistance to apoptosis is consistent with the antiapoptotic signature observed in MDMs exposed to gp120$_{IIIB}$ (8, 28), HIV-infected macrophages (47), macrophages/microglia serving as HIV reservoirs (48), and monocytes recovered from HIV-1-infected patients (27). Together, these results imply that regardless of whether gp120 originates from X4 or R5 strains, both are capable of inducing the overexpression of α7-nAChR in human macrophages that seem to be a distinctive element of HIV infection (8), chronic inflammation (49–52), and bacterial infection (53). Finally, the upregulation of α7-nAChR was not accompanied by any significant increase in *Egr1* levels during the first 24 h of incubation; therefore, there is still the possibility that it will experience changes later.

We focused our study on measuring α7-nAChR levels because this receptor is the cornerstone of CAR functioning in macrophages (5). In our studies we employed a specific antagonist (α-BuTX) of α7-nAChR, to measure its surface expression. Several nAChRs have been detected in murine macrophages, including α9-nAChR, which also recognizes α-BuTX; however, this receptor has not yet been identified in human macrophages (5, 54, 55). Conversely, α7-nAChR has been overwhelmingly identified in human macrophages from cell lines and primary cultures. Nonetheless, α9-nAChR must be studied in the future to rule out any participation in the gp120-induced upregulation of α7-nAChR in human macrophages or its expression itself. In summary, these results confirm previous observations regarding the α7-nAChR upregulation and substantially expand it through the evaluation of additional gp120s (gp120$_{JRFL}$ and gp120$_{ADA}$) from R5 HIV strains that use the CCR5 coreceptor to infect CD4-expressing cells.

The gp120$_{JRFL}$ used in this study has R5 tropism and binds to the CD4 receptor and CCR5 coreceptor (1) present in MDMs. To determine whether the α7-nAChR upregulation occurs *via* these receptors, CD4 and CCR5 were blocked with DIDS and maraviroc, respectively. Results showed that antagonizing CD4 and CCR5 significantly blocked the upregulation of α7-nAChR in MDMs. The reduction in α7-nAChR levels after blocking CD4 and CCR5 demonstrates that both compounds were able to avoid the interaction between gp120$_{JRFL}$ and these receptors, thus abrogating their respective activations and preventing α7-nAChR upregulation. Moreover, the fact that both compounds were able to significantly inhibit the upregulation of α7-nAChR suggests that both CD4 and CCR5 may be involved in the intracellular signaling that leads to the upregulation of α7-nAChR in human macrophages. This hypothesis is supported by studies demonstrating that RANTES enhancement of HIV replication in T-cells induces colocalization of CD4 and CXCR4 on immune cells, an effect that is also known to be triggered by gp120 (56–58) in CCR5-expressing cells (59). On the other hand, interestingly, the addition of two endogenous agonists produced by macrophages (60), RANTES and MIP-1β, just before addition of gp120$_{JRFL}$ substantially prevented the upregulation of α7-nAChR in MDMs to the levels found in the control cells (Fig. 2*B*). RANTES and MIP-1β are chemoattractant chemokines that play important roles in chronic and acute inflammation in uninfected subjects (61, 62), and inflammation is particularly elevated in HIV-infected subjects (63), mainly in the serum, lymph nodes, and cerebrospinal fluid (64–66). Results obtained in the current study are contrary to what has been observed for SDF-1α, a natural ligand of CXCR4, which

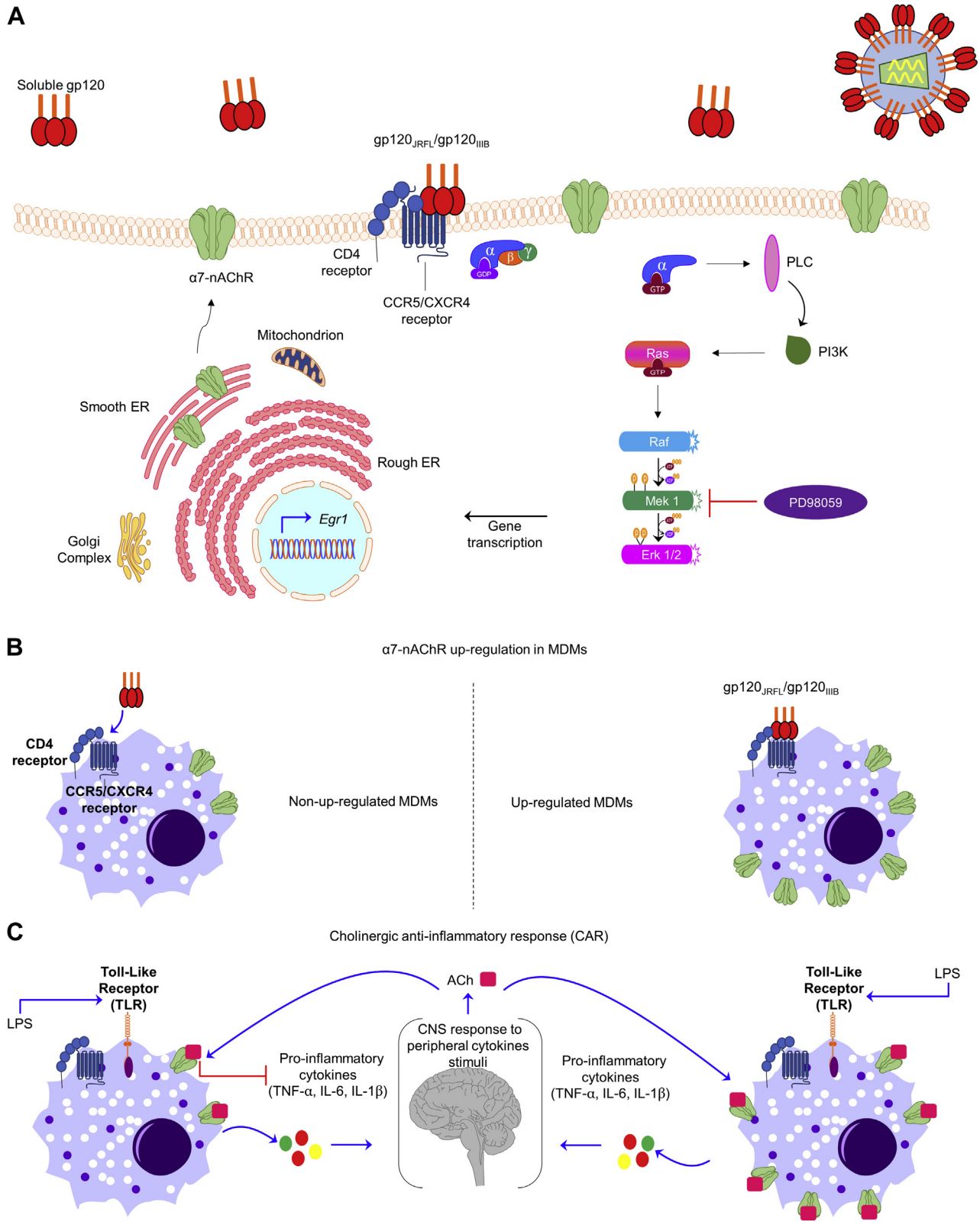

Figure 7. Proposed mechanism for gp120-induced upregulation of the α7-nAChR in MDMs. *A*, activation of CCR5 or CD4 by gp120$_{JRFL}$ causes activation of the Ras-Raf-MEK pathway that leads to modest activation of *Egr1*, a known transcription factor for the α7-nAChR gene (*CHRNA7*). *B*, the viral glycoprotein gp120$_{JRFL}$ induces the upregulation of α7-nAChRs. *C*, activation of the cholinergic anti-inflammatory response in macrophages demonstrates that gp120$_{JRFL}$ alters the macrophage phenotype, imparting a proinflammatory character because the activation of CAR is unable to reduce inflammatory cytokine levels.

has been reported to induce α7-nAChR upregulation in MDMs *in vitro* (8). Taken together, these results suggest that even though both gp120s promote similar upregulation of α7-nAChR, the stimulation of the CXCR4 and CCR5 coreceptors works differently as far as α7-nAChR upregulation in MDMs is concerned.

To dissect and better understand the mechanisms behind the upregulation of α7-nAChR induced by gp120$_{JRFL}$, MDMs were treated with PD98059 to determine if MAPK signaling was involved in transmitting the gp120$_{JRFL}$ signaling, which primarily leads to α7-nAChR upregulation. According to our results, the inhibition of MEK1 attenuated the upregulation of α7-nAChR induced by gp120$_{JRFL}$ but did not restore it to levels comparable to the control (Fig. 3*A*), suggesting that MEK1 may participate in the upregulation process but not all responses rely on this signaling molecule. Since PD98059 alone is capable of increasing α7-nAChR levels (Fig. 3*B*), it is possible that the expected inhibitory effect was masked by the stimulating action of PD98059 on α7-nAChR. Therefore, other signaling molecules could participate in this process (67). Overall, it cannot be ruled out that other proteins may contribute to the signaling that leads to α7-nAChR upregulation in MDMs, but MAPK signaling seems to be involved.

To further investigate the mechanisms that govern the upregulation of α7-nAChR in MDMs, we decided to evaluate whether there is any cross talk between CXCR4 and CCR5, the coreceptors used by gp120$_{IIIB}$ and gp120$_{JRFL}$/gp120$_{ADA}$, respectively, to upregulate α7-nAChR in MDMs. The CXCR4 coreceptor has previously been shown to participate in α7-nAChR upregulation once stimulated by gp120$_{IIIB}$ (8), but in the current study, we found that CCR5 stimulation is capable of inducing α7-nAChR upregulation once stimulated by gp120$_{JRFL}$ or gp120$_{ADA}$. Current results show that blocking of either CXCR4 or CCR5 does not influence the signaling of the other, resulting in upregulation of α7-nAChR (Fig. S5). That is, for example, even when CXCR4 is blocked, it does not prevent gp120$_{JRFL}$ from stimulating α7-nAChR upregulation through CCR5 activation. Consistent with this idea, the upregulation of α7-nAChR is not potentiated by the simultaneous addition of gp120$_{IIIB}$ and gp120$_{JRFL}$ (Fig. S5). In summary, the upregulation of α7-nAChR induced by g120$_{IIIB}$ or gp120$_{JRFL}$ does not involve cross talk between CXCR4 and CCR5. Also, these results suggest that upregulation mediated by gp120$_{JRFL}$ and gp120$_{ADA}$ recapitulates the cellular events that occur during the early stages of HIV infection with R5 tropic strains. On the other hand, the α7-nAChR upregulation induced by gp120$_{IIIB}$ can be indicative of the events observed in the chronic phase of the infection in which R5X4 and X4 strains are predominant (68).

HIV infection is characterized by the appearance of inflammatory processes that last throughout the patient's life. In the present work, similar to what was previously observed for gp120$_{IIIB}$ (8), gp120$_{JRFL}$ was able to induce the upregulation of α7-nAChR; however, it produced a different inflammation profile. Here, we show that gp120$_{JRFL}$ caused a CAR disruption for IL-6, GRO-α, and I-309, which is consistent with what was previously observed for gp120$_{IIIB}$ (8). However, here we found that CAR activation could reduce TNF-α levels successfully, something not observed in experiments performed with gp120$_{IIIB}$. This suggests that, although gp120$_{JRFL}$ produced a CAR disruption for some cytokines, activation of the CAR may still successfully reduce the levels of TNF-α in our experimental setting. Something similar was observed previously, but for MCP-1, a chemokine (8). Finally, gp120$_{JRFL}$ maintained levels of IL-10, an anti-inflammatory interleukin, similar to those produced by LPS alone, a finding contrary to what was observed in the case of gp120$_{IIIB}$, which stimulated a significant release of this anti-inflammatory molecule (8). This observation may imply that gp120$_{JRFL}$ may be more proinflammatory than is gp120$_{IIIB}$ because it does not allow a substantial release of IL-10 to counteract inflammation, although this does not seem always to be the case, at least for the chemokines (69). Our results show that the net phenotype of macrophages exposed to gp120$_{JRFL}$ is proinflammatory. In summary, gp120$_{JRFL}$ produces a CAR disruption for IL-6 and for the two chemokines evaluated (GRO-α and I-309). The CAR disruption detected here has serious implications in HIV-infected patients because it sheds light on cellular processes occurring in them that contribute to the chronic inflammation they experience. Another aspect that should not be ignored is the possibility that other immune cells expressing α7-nAChR play some role in the inflammatory alterations described above.

To counteract the proinflammatory effects caused by gp120$_{JRFL}$, MDMs were treated with bupropion, a partial α7-nAChR antagonist that (1) has proved to be safe for HIV-infected patients (70, 71), (2) has been used in HIV-infected patients (70, 72, 73), (3) does not interfere with antiretroviral therapy used by HIV-infected patients (71, 74), (4) exhibits anti-inflammatory properties (75–81), and (5) is FDA-approved (82). Those cytokines that did not respond to CAR activation were evaluated. Our results showed that bupropion effectively reduced the levels of IL-6, but not those of GRO-α and I-309. In summary, the application of bupropion proved to have limited anti-inflammatory action, thus underscoring the need for better medications focused on α7-nAChR to counteract HIV-induced inflammation.

Altogether, our findings suggest an important link between CCR5 and CD4 activation and the surface expression of the α7-nAChR in human macrophages. According to our results, these alterations cause CAR activity to be limited, which ends up contributing to the inflammation experienced by HIV-infected subjects. Undoubtedly, more research with a pharmacological approach is needed to rescue the activity of CAR under inflammation scenarios such as HIV infection. Moreover, this work demonstrates the complexity behind the upregulation of α7-nAChR induced by gp120$_{JRFL}$ and gp120$_{IIIB}$, which provides more avenues for research. The precise molecular mechanisms behind the upregulation of α7-nAChR in the presence of gp120 remain elusive. However, our results together with those of other groups suggest that chemokines (RANTES and MIP-1β) and gp120 may initiate both common and unique, ligand-specific signaling pathways. Indeed, signals induced by chemokine's binding to

correspondent receptors do not always mimic the interaction of the HIV-1 envelope with the chemokine receptors (83). Importantly, the relevance of restoring the CAR is not limited to the field of HIV but has important consequences in the recent pandemic caused by SARS CoV-2, the etiological agent causing COVID-19 in humans. Recent studies show that macrophages play a critical role in the appearance of the cytokine storm (84) and that α7-nAChR may be involved in this process (85). Furthermore, the strongest evidence of the role that α7-nAChR can have in this process is the amount of literature that has emerged showing that patients who self-administer nicotine (smokers) are less likely to have COVID-19, which has led the scientific community to consider therapeutic options including nicotine (86, 87), an agonist of α7-nAChRs. Certainly, the α7-nAChR expressed in human macrophages is emerging as an attractive pharmacological target to alleviate the extensive inflammation experienced by patients suffering from COVID-19.

Experimental procedures

Reagents and antibodies

Nicotine, RANTES, MIP-1β, 4,4′-diisothiocyanatostilbene-2,2′-disulfonic acid (DIDS), LPS, acetylcholine, bupropion, and maraviroc, were acquired from Sigma-Aldrich. Alexa-488 α-bungarotoxin was purchased from Invitrogen. gp120$_{JRFL}$ and gp120$_{ADA}$ were purchased from MyBioSource. gp120$_{IIIB}$ was from Fitzgerald Industries International. Monoclonal α7-nAChR antibody (Cat. # sc-5544, Santa Cruz Biotechnology), monoclonal GAPDH antibody (Cat. # ab8645, Abcam), and goat anti-mouse IgG HRP (Cat. # sc-2005, Santa Cruz Biotechnology) were obtained from Santa Cruz Biotechnology. An anti-goat secondary antibody-labeled HRP-conjugated were obtained from Sigma Aldrich (Cat. # AP307P, EMD Millipore).

Study subjects

All donors enrolled in this study signed the informed consent approved by the Institutional Committee for the Protection of Human Participants in Research (IRB number: 0910-033). All experiments were performed per University of Puerto Rico guidelines and regulations. Phlebotomy to obtain peripheral blood mononuclear cells was performed on healthy uninfected volunteer donors bled at the University of Puerto Rico, Río Piedras Campus for the studies depicted in all figures.

The human subject studies abide by the declaration of Helsinki Principles.

Cell culture of human monocyte-derived macrophages (MDMs)

Whole blood from all subjects was processed as described elsewhere (88) (Fig. S1*A*). Peripheral blood mononuclear cells were counted by a countless automated cell counter (Invitrogen) adjusted to 1–2 × 10^6 cells/ml and cultured into four-well Lab-Tek II Chambered Coverglass (Nalgene) for confocal microscopy. For western blots, 1.0 × 10^7–1.0 × 10^8 cells/ml were cultured in cell culture Petri dishes (Fisher Scientific) as previously described (88). For qRT-PCR, 1 × 10^7 cells per ml were cultured in six-well cell culture plates, and for ELISA 400 μL of the supernatant was obtained from 1 × 10^7 cells per ml seeded in 24-well cell culture plates were assayed (Corning CoStar). Monocytes were separated from lymphocytes by adherence. After separation, cells were differentiated for 7–8 days in RPMI-1640 supplemented with 20% inactivated fetal bovine serum, 10% inactivated human serum, and 1% PenStrep. All cultures were maintained at 37 °C with 5% CO_2. All experiments were performed with cells cultured from a single donor; blood or cells from different donors were not mixed. Cultures, buffers, and reagents were endotoxin-free. The HIV-1 glycoprotein gp120$_{IIIB}$ manufacturer certified that endotoxin levels were ≤100 EU/mg. The manufacturer of gp120$_{JRFL}$ and gp120$_{ADA}$ certified that endotoxin levels were <0.01 EU/μg as determined by LAL test. Also, for all of them, ≥95% purity was determined by sodium dodecyl sulfate–polyacrylamide gel electrophoresis.

Immunoblot

After treatment, MDMs were lysed using lysis buffer (mercaptoethanol diluted in phosphate-buffered saline [PBS 1×] to a final concentration of 2.5% and supplemented with a protease inhibitor cocktail [Thermo Scientific; pH 7.4]). Protein sample quantification was performed using an iMark Microplate Reader (BioRad). Total homogenate samples, 50 μg, were loaded onto a 10% polyacrylamide gel and run for 1 h at 30 V and then at 90 V until completion. After electrophoresis, gels were transferred to a PVDF membrane (Bio-Rad) using a wet system (Bio-Rad) for 2 h at 100 V. After this, membranes were incubated in a blocking solution (5% non-fat dry milk, Tris-buffered saline [TBS, 1×] for 1 h at room temperature). Subsequently, primary antibody incubation for α7-nAChR, diluted 1:200 (cat. No.: H-302; Santa Cruz Biotechnology), was performed overnight at 4 °C. After three to six consecutive washes (5 min each) with TBS-T 1× and a final wash with TBS (1×), an anti-goat secondary antibody labeled with horse-peroxidase-conjugated and diluted 1:2000 (cat. No.: AP307P; Millipore) was added and incubated for 1 h at room temperature. As a loading control, a mouse monoclonal [6C5] antibody for GAPDH diluted to 1:500 (cat. No.: ab8245; Abcam) was used. Membranes were processed using a chemiluminescence assay (Super Signal West Dura Extended Duration Substrate; Thermo Scientific) following the manufacturer's instructions. Molecular weight markers employed did not contain horseradish peroxidase; therefore, the image corresponding to the molecular weight markers lane was taken separately and eventually aligned with their respective immunoblots. Relative intensities of the blots were evaluated using Image Lab Image Capture and Analysis Software (Bio-Rad). The band quantifications are presented as the relative quantity of protein (experimental condition/untreated ratio).

Quantitative RT-PCR

Real-time PCR was performed following a previously described method with minor modifications (19). Total RNA samples were isolated from MDMs using the TRIzol Reagent

(Invitrogen Corporation). Possible genomic contamination from extracted RNA was treated with DNase using Ambion's DNA-free kit (Ambion). The RNA integrity was assayed in 1% electrophoresis agarose gel. Quantification of total RNA was performed using a NanoDrop system (Thermo). The cDNA synthesis was carried out using 2 μg of total RNA with the iScript cDNA Synthesis Kit (Bio-Rad Laboratories, Inc) following the manufacturer's instructions. Real-time PCR experiments were done using the iQ SYBR Green Supermix (Bio-Rad Laboratories, Inc) using a Mastercycler Ep realplex Thermal Cycler (Eppendorf, Hauppauge, NY), 10-μM concentration of forward and reverse primers. The following primer pairs were used: fwd=5′-GCTCTCTGCTCC TCCTGTTC-3′ and rev=5′-GACTCCGACCTTCACCTTCC-3′ for *GAPDH*, fwd=5′-AGCACCTTCAACCCTCA-3′ and rev= 5′-AGTCGAGTGGTTTGGCT-3′ for *Egr1*. Real-time qPCR was performed in a 25-μl reaction containing 12.5 μl SYBR Green PCR Master Mix (Bio-Rad), 1 μl of each primer (10 μM), 2 μl cDNA, and 8.5 μl water. PCR cycling conditions were 95 °C for 10 min followed by 45 cycles of 94 °C for 25 s, 60 °C for 25 s, and 72 °C for 40 s. Expression of *Egr1* was normalized to that of *GAPDH* using the *ddCt* method.

Confocal imaging

After differentiation, MDMs were incubated and maintained in media supplemented with either gp120$_{JRFL}$, or gp120$_{ADA}$ (both glycoproteins expressed in 293 cells), or full-length monomeric glycosylated gp120$_{IIIB}$ expressed in baculovirus, for 72 h. After incubation, the media was removed and MDMs were washed with PBS 1× (pH 7.4), followed by fixation with 4% formaldehyde for 15 min at room temperature, washed twice with PBS 1×, and labeled with Alexa-488-α-BuTX (Invitrogen) for 1 h at 70 μg/ml final concentration in buffer (NaCl, 120 mM; KCl, 4 mM; KH_2PO_4, 1.2 mM; $MgSO_4$, 1 mM; HEPES, 15 mM (pH 7.4); $CaCl_2$, 1 mM; bovine serum albumin, 2%; and glucose, 1%). After α-BuTX labeling, MDMs were washed with PBS 1× to remove unbound α-BuTX, followed by the addition of Mounting Media (H-1000, from Vector Labs Biotechnology Company) to be finally studied under confocal microscopes (Zeiss LSM Meta 510 and AR1 Nikon) at the Neuroimaging and Electrophysiology Facility (NIEF), Molecular Sciences Research Center (http://nief-upr.com). The remaining bound α-BuTX was excited at a wavelength of 488 nm (0.2%) using an Argon/2 laser, and its emission was acquired at 520 nm using a BP 505–550 filter, 64-μm pinhole using a Plan-Apochromat × 40/0.8M27 objective for experiments performed on Zeiss LSM Meta 510. For the experiments performed on AR1 Nikon, the excitation wavelength was 487.5 nm using an LU-N3 laser, and emission was acquired 525 nm using 450/50-550/50-595-50 filter, 24.27-μm pinhole using S Fluor 40× Oil DIC H N2 objective. Images were acquired by random snapshots at 2048 × 2048 dpi on Zeiss LSM 510 and at 1024 × 1024 dpi on AR1 Nikon followed by background subtractions. Relative fluorescence intensity analyses of each MDM were performed using the LSM 510 program or Nikon AR Nis Elements software. Each slide was analyzed generating five Z-stacks of confocal microscopy images (snapshots). Then, intensities were averaged for each cell and each snapshot. Relative intensities were averaged and plotted as a raw value unless otherwise specified in figure legends.

Nicotine competitive binding assay

The competitive binding assay was performed by adding nicotine to a final concentration of 500 μM before addition of Alexa-488-α-BuTX (2 μg/ml). MDMs were incubated for 15 min at 4 °C in the dark and washed with RPMI-1640 non-supplemented base. Cells were then fixed with 4% formaldehyde–PBS solution (pH 7.2) for 15 min at room temperature. After fixation, MDMs were washed three times with PBS 1× (pH 7.2). Finally, VectaShield (Vector Labs) was added for visualization and examination by confocal microscopy. Images were collected in Z-stacks at a magnification of 40× and analyzed. Three random snapshots were performed, and individual MDMs were analyzed for mean intensity and averaged.

Multiplex ELISA assay

Peripheral blood mononuclear cells from donors were cultured (7–8 days) in 24-well plates, differentiated into MDMs (Fig. S1*A*), and assayed for interleukins and chemokines production (IL-6, IL-10, TNF-α, GRO-α, and I-309) by Quansys Biosciences. After differentiation, media was changed for fresh media, and gp120$_{JRFL}$ was added for 72 h (to induce α7-nAChR upregulation), followed by three consecutive fresh media washes to remove gp120$_{JRFL}$. To study the cholinergic anti-inflammatory response, LPS was added as an inflammation inductor, according to the experimental condition tested. The cholinergic anti-inflammatory response experimental treatments consisted of LPS (100 ng/ml) challenges using *Escherichia coli* O111:B4 (Sigma), followed by the addition of ACh (30 μM). The acetylcholinesterase inhibitor pyridostigmine (1 mM) was added 10 min before the ACh application to avoid ACh hydrolysis. In the case of bupropion (70 ng/ml) containing assays, to partially antagonize α7-nAChR, bupropion was added 10 min before LPS or ACh application. For maraviroc (100 nM) containing assays, it was added as a cotreatment with LPS and/or ACh. Supernatants were collected 4-h posttreatment and stored at −80 °C for further analysis. All supernatants were sent to a contract laboratory (Quansys Biosciences, Logan, UT, USA) for cytokines quantification using the multiplex ELISA technology. Samples were analyzed in triplicate. Donors considered for each cytokine were independently evaluated, and those who did not exhibit CAR activity were not considered for analysis. A gp120$_{JRFL}$ control was included on each donor evaluated, and because cytokine induction was minimal, they were not plotted.

Basal calcium levels determination

After differentiation, MDMs were incubated and maintained in media supplemented with gp120$_{JRFL}$ for 72 h. After incubation with gp120, the media was removed and MDMs were washed with RPMI-1640 (fresh complete media), followed by

incubation with α-BuTX (100 nM) for 45 min to 1 h. After α-BuTX incubation, cells were washed twice with RPMI-1640 (no supplemented media/without fetal bovine serum (FBS) or human serum). Then RPMI-1640 was removed and cells were incubated with Fluo-4 AM in RPMI-1640 base, final concentration of 10 μM for 1 h in dark. After that, cells were washed twice with RPMI-1640 and kept in this solution to be finally studied under confocal microscopes (Zeiss LSM Meta 510) at the Neuroimaging and Electrophysiology Facility (NIEF), Molecular Sciences Research Center (http://nief-upr.com). Cells were excited at a wavelength of 488 nm (0.2%) using an Argon/2 laser, and its emission was acquired at 520 nm using a BP 505–550 filter, 64-μm pinhole using a Plan-Apochromat × 40/0.8M27 objective. Images were acquired by random snapshots at 2048 × 2048 dpi on Zeiss LSM 510 at 20× magnification followed by background subtractions.

Statistical analysis

All statistical analyses were performed using GraphPad (Graph Pad). For small sample sizes, nonparametric statistics were used. Wilcoxon signed-rank test was performed for paired analysis, comparisons between paired groups were made by using the Wilcoxon matched-pairs signed-rank test, and the one-sample *t*-test was used to compare a group mean to a hypothetical value=1. Quantitative variables are presented as a standard error of the mean (SEM) ± SD; a p-value < 0.05 was considered significant. Grubbs' test (alpha = 0.05) from GraphPad QuickCalcs, also called the ESD method (extreme studentized deviate), was used to determine outliers.

Data availability

All the data described is contained in the article and in the supporting information.

Supporting information—This article contains supporting information.

Acknowledgments—We thank Dr Manuel Delgado-Vélez for discussion and critical reading of the article. Special thanks to Mr Bismark Madera for the technical support with confocal microscopy at the Neuroimaging and Electrophysiology Facility (NIEF), http://www.nief-upr.com/. Without his contribution, a significant portion of this work would not have been possible.

This research was supported by the National Center for Research Resources (NCRR) Grant U54RR026139, the National Institute of Minority Health and Health Disparities (NIMHD) Grant 8U54MD007587-03, the National Institute of Neurological Disorders and Stroke (NINDS) Grant U54NS0430311, the National Institute of Mental Health (NIMH) Grant P30MH075673-07. Also, this research was supported by the National Institute of General Medical Sciences (NIGMS), University of Puerto Rico (UPR) Centers of Biomedical Research Excellence (COBRE) Neuroplasticity Center Grant P20GM103642. Infrastructure support was provided in part by the National Institute on Minority Health and Health Disparities Research Centers in Minority Institutions (RCMI) Grant 8G12MD007600. The content is solely the responsibility of the authors and does not necessarily represent the official views of the NIH.

Author contributions—S. C. R. is responsible for the conceptualization of the study, carrying out the experiments, and writing the manuscript. J. O. C. S. collaborated in the experimental design, data analysis, and the preparation of the manuscript. O. Q. provided support and contributed to the design of the experiments and data analysis. K. Q. F. contributed to data analysis. J. A. L. D. coordinated the team efforts and contributed to the manuscript preparation. All authors reviewed the results and approved the final version of the manuscript.

Funding and additional information—S. C. R. was supported by the RISE-MBRS-NIH Program (2R25GM061151).

Conflict of interest—The authors declare that they have no conflicts of interest with the contents of this article.

Abbreviations—The abbreviations used are: ACh, acetylcholine; α-BuTX, alpha bungarotoxin; CAR, cholinergic anti-inflammatory response.

References

1. Berger, E. A., Murphy, P. M., and Farber, J. M. (1999) Chemokine receptors as HIV-1 coreceptors: Roles in viral entry, tropism, and disease. *Annu. Rev. Immunol.* **17**, 657–700
2. Goodenow, M. M., and Collman, R. G. (2006) HIV-1 coreceptor preference is distinct from target cell tropism: A dual-parameter nomenclature to define viral phenotypes. *J. Leukoc. Biol.* **80**, 965–972
3. Brumme, Z. L., Henrick, B. M., Brumme, C. J., Hogg, R. S., Montaner, J. S. G., and Harrigan, P. R. (2005) Short communication. Association of the CCR5delta32 mutation with clinical response and >5-year survival following initiation of first triple antiretroviral regimen. *Antivir. Ther.* **10**, 849–853
4. Rana, S., Besson, G., Cook, D. G., Rucker, J., Smyth, R. J., Yi, Y., Turner, J. D., Guo, H. H., Du, J. G., Peiper, S. C., Lavi, E., Samson, M., Libert, F., Liesnard, C., Vassart, G., *et al.* (1997) Role of CCR5 in infection of primary macrophages and lymphocytes by macrophage-tropic strains of human immunodeficiency virus: Resistance to patient-derived and prototype isolates resulting from the delta ccr5 mutation. *J. Virol.* **71**, 3219–3227
5. Wang, H., Yu, M., Ochani, M., Amella, C. A., Tanovic, M., Susarla, S., Li, J. H., Wang, H., Yang, H., Ulloa, L., Al-Abed, Y., Czura, C. J., and Tracey, K. J. (2003) Nicotinic acetylcholine receptor alpha7 subunit is an essential regulator of inflammation. *Nature* **421**, 384–388
6. Pavlov, V. A., and Tracey, K. J. (2006) Controlling inflammation: The cholinergic anti-inflammatory pathway. *Biochem. Soc. Trans.* **34**, 1037–1040
7. Borovikova, L. V., Ivanova, S., Zhang, M., Yang, H., Botchkina, G. I., Watkins, L. R., Wang, H., Abumrad, N., Eaton, J. W., and Tracey, K. J. (2000) Vagus nerve stimulation attenuates the systemic inflammatory response to endotoxin. *Nature* **405**, 458–462
8. Delgado-Vélez, M., Báez-Pagán, C. A., Gerena, Y., Quesada, O., Santiago-Pérez, L. I., Capó-Vélez, C. M., Wojna, V., Meléndez, L., León-Rivera, R., Silva, W., and Lasalde-Dominicci, J. A. (2015) The α7-nicotinic receptor is upregulated in immune cells from HIV-seropositive women: Consequences to the cholinergic anti-inflammatory response. *Clin. Transl. Immunol.* **4**, e53
9. Delgado-Vélez, M., and Lasalde-Dominicci, J. A. (2018) The cholinergic anti-inflammatory response and the role of macrophages in HIV-induced inflammation. *Int. J. Mol. Sci.* **19**, 1473
10. Klasse, P. J., and Moore, J. P. (2004) Is there enough gp120 in the body fluids of HIV-1-infected individuals to have biologically significant effects? *Virology* **323**, 1–8
11. Gilbert, M., Kirihara, J., and Mills, J. (1991) Enzyme-linked immunoassay for human immunodeficiency virus type 1 envelope glycoprotein 120. *J. Clin. Microbiol.* **29**, 142–147

12. Oh, S. K., Cruikshank, W. W., Raina, J., Blanchard, G. C., Adler, W. H., Walker, J., and Kornfeld, H. (1992) Identification of HIV-1 envelope glycoprotein in the serum of AIDS and ARC patients. *J. Acquir. Immune Defic. Syndr.* **5**, 251–256
13. Santosuosso, M., Righi, E., Lindstrom, V., Leblanc, P. R., and Poznansky, M. C. (2009) HIV-1 envelope protein gp120 is present at high concentrations in secondary lymphoid organs of individuals with chronic HIV-1 infection. *J. Infect. Dis.* **200**, 1050–1053
14. Raff, H. V., Picker, L. J., and Stobo, J. D. (1980) Macrophage heterogeneity in man. A subpopulation of HLA-DR-bearing macrophages required for antigen-induced T cell activation also contains stimulators for autologous-reactive T cells. *J. Exp. Med.* **152**, 581–593
15. Witsell, A. L., and Schook, L. B. (1991) Macrophage heterogeneity occurs through a developmental mechanism. *Proc. Natl. Acad. Sci. U. S. A.* **88**, 1963–1967
16. Gordon, S., and Taylor, P. R. (2005) Monocyte and macrophage heterogeneity. *Nat. Rev. Immunol.* **5**, 953–964
17. Yi, Y., Isaacs, S. N., Williams, D. A., Frank, I., Schols, D., De Clercq, E., Kolson, D. L., and Collman, R. G. (1999) Role of CXCR4 in cell-cell fusion and infection of monocyte-derived macrophages by primary human immunodeficiency virus type 1 (HIV-1) strains: Two distinct mechanisms of HIV-1 dual tropism. *J. Virol.* **73**, 7117–7125
18. Luo, Y., Lathia, J., Mughal, M., and Mattson, M. P. (2008) SDF1α/CXCR4 signaling, via ERKs and the transcription factor Egr1, induces expression of a 67-kDa form of glutamic acid decarboxylase in embryonic hippocampal neurons. *J. Biol. Chem.* **283**, 24789–24800
19. Ballester, L. Y., Capó-Vélez, C. M., García-Beltrán, W. F., Ramos, F. M., Vázquez-Rosa, E., Ríos, R., Mercado, J. R., Meléndez, R. I., and Lasalde-Dominicci, J. A. (2012) Up-regulation of the neuronal nicotinic receptor α7 by HIV glycoprotein 120: Potential implications for HIV-associated neurocognitive disorder. *J. Biol. Chem.* **287**, 3079–3086
20. Criado, M., Domínguez del Toro, E., Carrasco-Serrano, C., Smillie, F. I., Juíz, J. M., Viniegra, S., and Ballesta, J. J. (1997) Differential expression of alpha-bungarotoxin-sensitive neuronal nicotinic receptors in adrenergic chromaffin cells: A role for transcription factor Egr-1. *J. Neurosc.* **17**, 6554–6564
21. Crews, C. M., Alessandrini, A., and Erikson, R. L. (1992) The primary structure of MEK, a protein kinase that phosphorylates the ERK gene product. *Science* **258**, 478–480
22. Capó-Vélez, C. M., Morales-Vargas, B., García-González, A., Grajales-Reyes, J. G., Delgado-Vélez, M., Madera, B., Báez-Pagán, C. A., Quesada, O., and Lasalde-Dominicci, J. A. (2018) The alpha7-nicotinic receptor contributes to gp120-induced neurotoxicity: Implications in HIV-associated neurocognitive disorders. *Sci. Rep.* **8**, 1829
23. Haughey, N. J., and Mattson, M. P. (2002) Calcium dysregulation and neuronal apoptosis by the HIV-1 proteins Tat and gp120. *J. Acquir. Immune Defic. Syndr. 1999* **31 Suppl 2**, S55–S61
24. Liu, Q. H., Williams, D. A., McManus, C., Baribaud, F., Doms, R. W., Schols, D., De Clercq, E., Kotlikoff, M. I., Collman, R. G., and Freedman, B. D. (2000) HIV-1 gp120 and chemokines activate ion channels in primary macrophages through CCR5 and CXCR4 stimulation. *Proc. Natl. Acad. Sci. U. S. A.* **97**, 4832–4837
25. Lee, C., Liu, Q.-H., Tomkowicz, B., Yi, Y., Freedman, B. D., and Collman, R. G. (2003) Macrophage activation through CCR5- and CXCR4-mediated gp120-elicited signaling pathways. *J. Leukoc. Biol.* **74**, 676–682
26. Cummins, N. W., and Badley, A. D. (2013) Anti-apoptotic mechanisms of HIV: Lessons and novel approaches to curing HIV. *Cell. Mol. Life Sci.* **70**, 3355–3363
27. Giri, M. S., Nebozyhn, M., Raymond, A., Gekonge, B., Hancock, A., Creer, S., Nicols, C., Yousef, M., Foulkes, A. S., Mounzer, K., Shull, J., Silvestri, G., Kostman, J., Collman, R. G., Showe, L., *et al.* (2009) Circulating monocytes in HIV-1-infected viremic subjects exhibit an anti-apoptosis gene signature and virus- and host-mediated apoptosis resistance. *J. Immunol.* **182**, 4459–4470
28. Yuan, Z., Fan, X., Staitieh, B., Bedi, C., Spearman, P., Guidot, D. M., and Sadikot, R. T. (2017) HIV-related proteins prolong macrophage survival through induction of Triggering receptor expressed on myeloid cells-1. *Sci. Rep.* **7**, 42028
29. Stacey, A. R., Norris, P. J., Qin, L., Haygreen, E. A., Taylor, E., Heitman, J., Lebedeva, M., DeCamp, A., Li, D., Grove, D., Self, S. G., and Borrow, P. (2009) Induction of a striking systemic cytokine cascade prior to peak viremia in acute human immunodeficiency virus type 1 infection, in contrast to more modest and delayed responses in acute hepatitis B and C virus infections. *J. Virol.* **83**, 3719–3733
30. Kedzierska, K., and Crowe, S. M. (2001) Cytokines and HIV-1: Interactions and clinical implications. *Antivir. Chem. Chemother.* **12**, 133–150
31. Hoover, D. B. (2017) Cholinergic modulation of the immune system presents new approaches for treating inflammation. *Pharmacol. Ther.* **179**, 1–16
32. Slemmer, J. E., Martin, B. R., and Damaj, M. I. (2000) Bupropion is a nicotinic antagonist. *J. Pharmacol. Exp. Ther.* **295**, 321–327
33. Fryer, J. D., and Lukas, R. J. (1999) Noncompetitive functional inhibition at diverse, human nicotinic acetylcholine receptor subtypes by bupropion, phencyclidine, and ibogaine. *J. Pharmacol. Exp. Ther.* **288**, 88–92
34. Moyle, G. J., Wildfire, A., Mandalia, S., Mayer, H., Goodrich, J., Whitcomb, J., and Gazzard, B. G. (2005) Epidemiology and predictive factors for chemokine receptor use in HIV-1 infection. *J. Infect. Dis.* **191**, 866–872
35. Wang, J., Alvarez, R., Roderiquez, G., Guan, E., and Norcross, M. A. (2004) Constitutive association of cell surface CCR5 and CXCR4 in the presence of CD4. *J. Cell. Biochem.* **93**, 753–760
36. Hileman, C. O., and Funderburg, N. T. (2017) Inflammation, immune activation, and antiretroviral therapy in HIV. *Curr. HIV/AIDS Rep.* **14**, 93–100
37. Massanella, M., Fromentin, R., and Chomont, N. (2016) Residual inflammation and viral reservoirs: Alliance against an HIV cure. *Curr. Opin. HIV AIDS* **11**, 234–241
38. Drisdel, R. C., Manzana, E., and Green, W. N. (2004) The role of palmitoylation in functional expression of nicotinic alpha7 receptors. *J. Neurosci.* **24**, 10502–10510
39. Alexander, J. K., Sagher, D., Krivoshein, A. V., Criado, M., Jefford, G., and Green, W. N. (2010) Ric-3 promotes alpha7 nicotinic receptor assembly and trafficking through the ER subcompartment of dendrites. *J. Neurosci.* **30**, 10112–10126
40. Murakami, K., Ishikawa, Y., and Sato, F. (2013) Localization of α7 nicotinic acetylcholine receptor immunoreactivity on GABAergic interneurons in layers I-III of the rat retrosplenial granular cortex. *Neuroscience* **252**, 443–459
41. King, J. R., Ullah, A., Bak, E., Jafri, M. S., and Kabbani, N. (2018) Ionotropic and metabotropic mechanisms of allosteric modulation of α7 nicotinic receptor intracellular calcium. *Mol. Pharmacol.* **93**, 601–611
42. Kabbani, N., and Nichols, R. A. (2018) Beyond the channel: Metabotropic signaling by nicotinic receptors. *Trends Pharmacol. Sci.* **39**, 354–366
43. King, J. R., Gillevet, T. C., and Kabbani, N. (2017) A G protein-coupled α7 nicotinic receptor regulates signaling and TNF-α release in microglia. *FEBS Open Bio* **7**, 1350–1361
44. Razani-Boroujerdi, S., Boyd, R. T., Dávila-García, M. I., Nandi, J. S., Mishra, N. C., Singh, S. P., Pena-Philippides, J. C., Langley, R., and Sopori, M. L. (2007) T cells express alpha7-nicotinic acetylcholine receptor subunits that require a functional TCR and leukocyte-specific protein tyrosine kinase for nicotine-induced Ca2+ response. *J. Immunol.* **179**, 2889–2898
45. de Jonge, W. J., and Ulloa, L. (2007) The alpha7 nicotinic acetylcholine receptor as a pharmacological target for inflammation. *Br. J. Pharmacol.* **151**, 915–929
46. Thomsen, M. S., and Mikkelsen, J. D. (2012) The α7 nicotinic acetylcholine receptor complex: One, two or multiple drug targets? *Curr. Drug Targets* **13**, 707–720
47. Swingler, S., Mann, A. M., Zhou, J., Swingler, C., and Stevenson, M. (2007) Apoptotic killing of HIV-1-infected macrophages is subverted by the viral envelope glycoprotein. *PLoS Pathog.* **3**, 1281–1290
48. Castellano, P., Prevedel, L., and Eugenin, E. A. (2017) HIV-infected macrophages and microglia that survive acute infection become viral reservoirs by a mechanism involving Bim. *Sci. Rep.* **7**, 12866
49. Chernyavsky, A. I., Arredondo, J., Skok, M., and Grando, S. A. (2010) Auto/paracrine control of inflammatory cytokines by acetylcholine in

macrophage-like U937 cells through nicotinic receptors. *Int. Immunopharmacol.* **10**, 308–315
50. Cedillo, J. L., Arnalich, F., Martín-Sánchez, C., Quesada, A., Rios, J. J., Maldifassi, M. C., Atienza, G., Renart, J., Fernández-Capitán, C., García-Rio, F., López-Collazo, E., and Montiel, C. (2015) Usefulness of α7 nicotinic receptor messenger RNA levels in peripheral blood mononuclear cells as a marker for cholinergic antiinflammatory pathway activity in septic patients: Results of a pilot study. *J. Infect. Dis.* **211**, 146–155
51. Khan, M. A. S., Farkhondeh, M., Crombie, J., Jacobson, L., Kaneki, M., and Martyn, J. A. J. (2012) Lipopolysaccharide upregulates α7 acetylcholine receptors: Stimulation with GTS-21 mitigates growth arrest of macrophages and improves survival in burned mice. *Shock* **38**, 213–219
52. Zanetti, S. R., Ziblat, A., Torres, N. I., Zwirner, N. W., and Bouzat, C. (2016) Expression and functional role of α7 nicotinic receptor in human cytokine-stimulated NK cells. *J. Biol. Chem.* **291**, 16541–16552
53. Islas-Weinstein, L., Marquina-Castillo, B., Mata-Espinosa, D., Paredes-González, I. S., Chávez, J., Balboa, L., Marín Franco, J. L., Guerrero-Romero, D., Barrios-Payan, J. A., and Hernandez-Pando, R. (2020) The cholinergic system contributes to the immunopathological progression of experimental pulmonary tuberculosis. *Front. Immunol.* **11**, 581911
54. Siniavin, A. E., Streltsova, M. A., Kudryavtsev, D. S., Shelukhina, I. V., Utkin, Y. N., and Tsetlin, V. I. (2020) Activation of α7 nicotinic acetylcholine receptor upregulates HLA-DR and macrophage receptors: Potential role in adaptive immunity and in preventing immunosuppression. *Biomolecules* **10**, 507
55. Padilla, A., Keating, P., Hartmann, J. X., and Marí, F. (2017) Effects of α-conotoxin ImI on TNF-α, IL-8 and TGF-β expression by human macrophage-like cells derived from THP-1 pre-monocytic leukemic cells. *Sci. Rep.* **7**, 12742
56. Iyengar, S., Hildreth, J. E., and Schwartz, D. H. (1998) Actin-dependent receptor colocalization required for human immunodeficiency virus entry into host cells. *J. Virol.* **72**, 5251–5255
57. Ugolini, S., Moulard, M., Mondor, I., Barois, N., Demandolx, D., Hoxie, J., Brelot, A., Alizon, M., Davoust, J., and Sattentau, Q. J. (1997) HIV-1 gp120 induces an association between CD4 and the chemokine receptor CXCR4. *J. Immunol.* **159**, 3000–3008
58. Lapham, C. K., Ouyang, J., Chandrasekhar, B., Nguyen, N. Y., Dimitrov, D. S., and Golding, H. (1996) Evidence for cell-surface association between fusin and the CD4-gp120 complex in human cell lines. *Science* **274**, 602–605
59. Xiao, X., Kinter, A., Broder, C. C., and Dimitrov, D. S. (2000) Interactions of CCR5 and CXCR4 with CD4 and gp120 in human blood monocyte-derived dendritic cells. *Exp. Mol. Pathol.* **68**, 133–138
60. Dorner, B. G., Scheffold, A., Rolph, M. S., Huser, M. B., Kaufmann, S. H. E., Radbruch, A., Flesch, I. E. A., and Kroczek, R. A. (2002) MIP-1alpha, MIP-1beta, RANTES, and ATAC/lymphotactin function together with IFN-gamma as type 1 cytokines. *Proc. Natl. Acad. Sci. U. S. A.* **99**, 6181–6186
61. Conti, P., and DiGioacchino, M. (2001) MCP-1 and RANTES are mediators of acute and chronic inflammation. *Allergy Asthma Proc.* **22**, 133–137
62. Gingo, M. R., Wenzel, S. E., Steele, C., Kessinger, C. J., Lucht, L., Lawther, T., Busch, M., Hillenbrand, M. E., Weinman, R., Slivka, W. A., McMahon, D. K., Zhang, Y., Sciurba, F. C., and Morris, A. (2012) Asthma diagnosis and airway bronchodilator response in HIV-infected patients. *J. Allergy Clin. Immunol.* **129**, 708–714.e8
63. Malnati, M. S., Tambussi, G., Clerici, E., Polo, S., Algeri, M., Nardese, V., Furci, L., Lazzarin, A., and Lusso, P. (1997) Increased plasma levels of the C-C chemokine RANTES in patients with primary HIV-1 infection. *J. Biol. Regul. Homeost. Agents* **11**, 40–42
64. De Almeida, S. M., Rotta, I., Jiang, Y., Li, X., Raboni, S. M., Ribeiro, C. E., Smith, D., Potter, M., Vaida, F., Letendre, S., and Ellis, R. J. (2016) Biomarkers of chemotaxis and inflammation in cerebrospinal fluid and serum in individuals with HIV-1 subtype C versus B. *J. Neurovirol.* **22**, 715–724
65. de Almeida, S. M., Rotta, I., Ribeiro, C. E., Oliveira, M. F., Chaillon, A., de Pereira, A. P., Cunha, A. P., Zonta, M., Bents, J. F., Raboni, S. M., Smith, D., Letendre, S., and Ellis, R. J. (2017) Dynamic of CSF and serum biomarkers in HIV-1 subtype C encephalitis with CNS genetic compartmentalization- case study. *J. Neurovirol.* **23**, 460–473
66. Trumpfheller, C., Tenner-Racz, K., Racz, P., Fleischer, B., and Frosch, S. (1998) Expression of macrophage inflammatory protein (MIP)-1α, MIP-1β, and RANTES genes in lymph nodes from HIV+ individuals: Correlation with a Th1-type cytokine response. *Clin. Exp. Immunol.* **112**, 92–99
67. Zdanowski, R., Krzyżowska, M., Ujazdowska, D., Lewicka, A., and Lewicki, S. (2015) Role of α7 nicotinic receptor in the immune system and intracellular signaling pathways. *Cent. Eur. J. Immunol.* **40**, 373–379
68. Regoes, R. R., and Bonhoeffer, S. (2005) The HIV coreceptor switch: A population dynamical perspective. *Trends Microbiol.* **13**, 269–277
69. Fantuzzi, L., Canini, I., Belardelli, F., and Gessani, S. (2001) HIV-1 gp120 stimulates the production of β-chemokines in human peripheral blood monocytes through a CD4-independent mechanism. *J. Immunol.* **166**, 5381–5387
70. Currier, M. B., Molina, G., and Kato, M. (2003) A prospective trial of sustained-release bupropion for depression in HIV-seropositive and AIDS patients. *Psychosomatics* **44**, 120–125
71. Pedrol-Clotet, E., Deig-Comerma, E., Ribell-Bachs, M., Vidal-Castell, I., García-Rodríguez, P., and Soler, A. (2006) [Bupropion use for smoking cessation in HIV-infected patients receiving antiretroviral therapy]. *Enferm. Infecc. Microbiol. Clin.* **24**, 509–511
72. Park-Wyllie, L. Y., and Antoniou, T. (2003) Concurrent use of bupropion with CYP2B6 inhibitors, nelfinavir, ritonavir and efavirenz: A case series. *AIDS* **17**, 638–640
73. Shahrir, S., Crothers, K., McGinnis, K. A., Chan, K. C. G., Baeten, J. M., Wilson, S. M., Butt, A. A., Pisani, M. A., Baldassarri, S. R., Justice, A., and Williams, E. C. (2020) Receipt and predictors of smoking cessation pharmacotherapy among veterans with and without HIV. *Prog. Cardiovasc. Dis.* **63**, 118–124
74. Drach, L., Holbert, T., Maher, J., Fox, V., Schubert, S., and Saddler, L. C. (2010) Integrating smoking cessation into HIV care. *AIDS Patient Care STDs* **24**, 139–140
75. Altschuler, E. L., and Kast, R. E. (2003) Bupropion in psoriasis and atopic dermatitis: Decreased tumor necrosis factor-alpha? *Psychosom. Med.* **65**, 719
76. Kast, R. E. (2003) Anti- and pro-inflammatory considerations in antidepressant use during medical illness: Bupropion lowers and mirtazapine increases circulating tumor necrosis factor-alpha levels. *Gen. Hosp. Psychiatry* **25**, 495–496
77. Kane, S., Altschuler, E. L., and Kast, R. E. (2003) Crohn's disease remission on bupropion. *Gastroenterology* **125**, 1290
78. Brustolim, D., Ribeiro-dos-Santos, R., Kast, R. E., Altschuler, E. L., and Soares, M. B. P. (2006) A new chapter opens in anti-inflammatory treatments: The antidepressant bupropion lowers production of tumor necrosis factor-alpha and interferon-gamma in mice. *Int. Immunopharmacol.* **6**, 903–907
79. Cámara-Lemarroy, C. R., Guzmán-de la Garza, F. J., Cordero-Pérez, P., Alarcón-Galván, G., Ibarra-Hernández, J. M., Muñoz-Espinosa, L. E., and Fernández-Garza, N. E. (2013) Bupropion reduces the inflammatory response and intestinal injury due to ischemia-reperfusion. *Transpl. Proc.* **45**, 2502–2505
80. Maciel, I. S., Silva, R. B. M., Morrone, F. B., Calixto, J. B., and Campos, M. M. (2013) Synergistic effects of celecoxib and bupropion in a model of chronic inflammation-related depression in mice. *PLoS One* **8**, e77227
81. Rashidian, A., Dejban, P., Karami Fard, K., Abdollahi, A., Chamanara, M., Dehpour, A., and Hasanvand, A. (2020) Bupropion ameliorates acetic acid-induced colitis in rat: The involvement of the TLR4/NF-kB signaling pathway. *Inflammation* **43**, 1999–2009
82. Huecker, M. R., Smiley, A., and Saadabadi, A. (2020) Bupropion *StatPearls*. StatPearls Publishing, Treasure Island, FL
83. Popik, W., and Pitha, P. M. (2000) Exploitation of cellular signaling by HIV-1: Unwelcome guests with master keys that signal their entry. *Virology* **276**, 1–6
84. Merad, M., and Martin, J. C. (2020) Pathological inflammation in patients with COVID-19: A key role for monocytes and macrophages. *Nat. Rev. Immunol.* **20**, 355–362

85. Anderson, G., and Reiter, R. J. (2020) Covid-19 pathophysiology: Interactions of gut microbiome, melatonin, vitamin D, stress, kynurenine and the alpha 7 nicotinic receptor. Treatment implications. *Melatonin Res.* **3**, 322–345
86. Farsalinos, K., Barbouni, A., and Niaura, R. (2020) Systematic review of the prevalence of current smoking among hospitalized COVID-19 patients in China: Could nicotine be a therapeutic option? *Intern. Emerg. Med.* **15**, 845–852
87. Tindle, H. A., Newhouse, P. A., and Freiberg, M. S. (2020) Beyond smoking cessation: Investigating medicinal nicotine to prevent and treat COVID-19. *Nicotine Tob. Res.* **22**, 1669–1670
88. Delgado-Vélez, M., Lugo-Chinchilla, A., Lizardo, L., Morales, I., Robles, Y., Bruno, N., Rodríguez, J. W., Ríos-Olivares, E., Correa, M., and Renaud, F. L. (2008) Chronic exposure of human macrophages *in vitro* to morphine and methadone induces a putative tolerant/dependent state. *J. Neuroimmunol.* **196**, 94–100